

Missing short-range interactions in the hydrogen bond of compressed ice

Yongli Huang,¹ Zengsheng Ma¹, Xi Zhang,^{2,3} Guanghui Zhou,⁴ Yichun Zhou,¹ and Chang Q Sun^{1,2,*}

¹ Key Laboratory of Low-dimensional Materials and Application Technology, Ministry of Education, and Faculty of Materials, Optoelectronics and Physics, Xiangtan University, Xiangtan, 411105, China

² School of Electrical and Electronic Engineering, Nanyang Technological University, Singapore 639798

³ College of Materials Science and Engineering, China Jiliang University, Hangzhou 310018, China

⁴ Department of Physics and Key Laboratory for Low-Dimensional Structures and Quantum Manipulation (Ministry of Education), Hunan Normal University, Changsha, 410081, China

Combining the Lagrangian-Laplace mechanics and the known pressure dependence of the length-stiffness relaxation dynamics, we have determined the critical, yet often-overlooked, short-range interactions in the O:H–O hydrogen bond of compressed ice. This approach has enabled determination of the force constant, cohesive energy, potential energy of the O:H and the H–O segment at each quasi-equilibrium state as well as their pressure dependence. Evidencing the essentiality of the inter-electron-pair Coulomb repulsion and the segmental strength disparity in determining the asymmetric O:H–O relaxation dynamics and the anomalous properties of ice, results confirmed that compression shortens and stiffens the O:H bond and meanwhile lengthens and softens the H–O bond.

*SI is accompanied.

PACS numbers: 61.20.Ja, 61.30.Hn, 68.08.Bc

Water and ice has attracted much attention because of its anomalous performance relating to issues from galaxy to geology, climate, biology, and to our daily lives [1-7]. As the building unit, the hydrogen bond (O:H–O)[8] relaxes in different manners under the change of environment conditions, which determines the anomalous properties of water and ice. Contributions have been made experimentally [9-11], computationally [12-16], and theoretically [17, 18] to the understanding of water and ice based on the polarizable or non-polarizable models [19, 20], including the TIP n P (n varies from 1 to 5) series [19-23]. Using *ab initio* density functional theory and molecular dynamics calculations, one is able to reproduce some of the anomalies demonstrated by compressed ice with limited knowledge about the nature of the inter- and intra-molecular interactions [24].

The objective of this work is to explore analytically the energy relaxation dynamics of the segmented O:H–O bond of ice under compression based on the Lagrangian-Laplace mechanics [25-27]. With the known length-stiffness relaxation dynamics of the O:H–O bond under compression [3-6] as input, we have been able to determine the force constants, the potential well depths, and the cohesive energies of each part of the O:H–O bond as well as their pressure dependence.

A linear hydrogen bond is assumed for simplicity because the O:H–O bond angle in ice is valued at $170 \pm 4^\circ$ [28]. By averaging the surrounding background interactions of H₂O molecules and protons and the nuclear quantum effect on fluctuations [29], we focus on the short-range interactions in this O:H–O bond with H being the coordination origin. As illustrated in Figure 1, the van der Waals force is limited to the O:H bond (denoted L) [30], the exchange interaction is within the H–O polar-covalent bond (denoted H) [31], and the Coulomb repulsion (denoted C) applies between the electron pairs attached to the adjacent oxygen ions, see Supplementary information (SI) [32].

Because of the short-range nature of the interactions, only the solid lines in the shaded area in Figure

1 are effective for the basic O:H–O unit. These interactions will switch off immediately outside the O:H–O region. These interactions determine the physical properties irrespective of the phase structures of the hydrogen-bonded networks but only O—O interaction bridged by H. The presence of inter-electron-pair Coulomb repulsion dislocates both O ions slightly away from their respective equilibrium position. Δ_x ($x = L$ for the O:H and $x = H$ for the H–O bond) denotes the dislocations. d_{x0} is the interionic distance at equilibrium without the Coulomb repulsion being involved. $d_x = d_{x0} + \Delta_x$ is the quasi-equilibrium bond length with the Coulomb repulsion being involved. The Coulomb repulsion raises the cohesive energies of the O:H and the H–O from E_{x0} to E_x by the same amount.

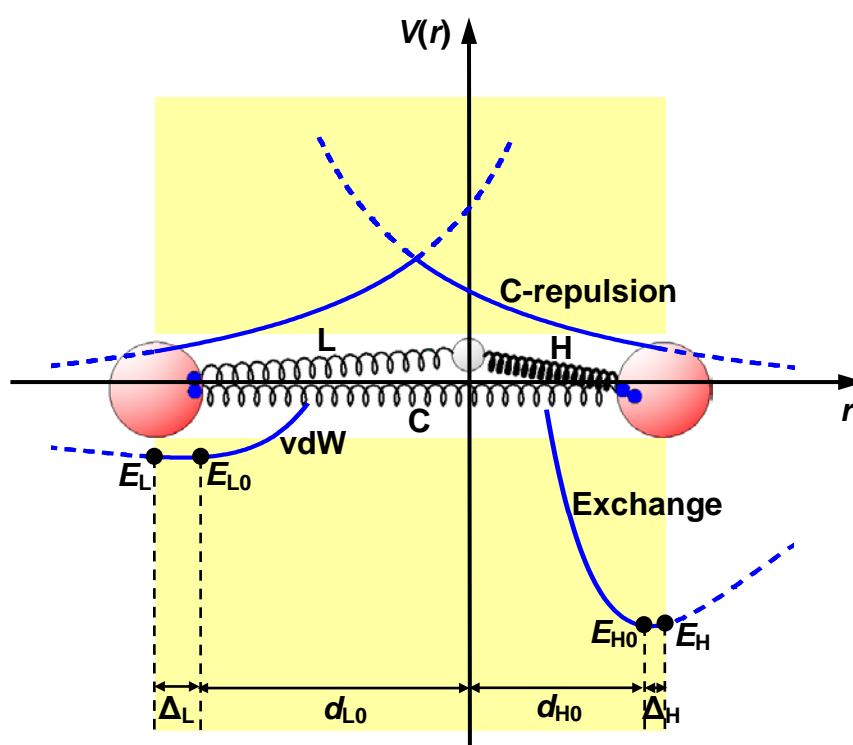


Figure 1 Schematic of the segmented O:H–O bond with springs representing the short-range interactions with H atom being the coordination origin: intramolecular exchange interaction limited to the H–O bond (H), intermolecular van der Waals (vdW) force limited to the O:H bond (L), and the inter-electron-pair Coulomb repulsion (C-repulsion) force between adjacent O—O (C). The red and grey spheres denote the oxygen and the hydrogen atoms, respectively. The pairs of dots on oxygen

denote the electron pairs (lone pair and bonding pair). The Coulomb repulsion pushes both O atoms away from their equilibrium positions.

The O:H-O bond is taken as two oscillators coupled by Coulomb interaction. The reduced mass of the H₂O:H₂O oscillator is $m_L=18 \times 18 / (18+18)m_0 = 9m_0$ and that of the H-O oscillator is $m_H = 1 \times 16 / (1+16)m_0 = 16/17 m_0$ with m_0 being the unit mass of 1.66×10^{-27} kg. The O:H-O bond motion follows the Lagrangian motion equation [25]:

$$\frac{d}{dt} \left(\frac{\partial L}{\partial (dq_i/dt)} \right) - \frac{\partial L}{\partial q_i} = Q_i \quad (1)$$

The Lagrangian $L = T - V$ consists of the total kinetic energy T and the total potential energy V . Q_i denotes the generalized non-conservative forces. Here, it is the pressure f_P . The time-dependent $q_i(t)$ represents the generalized variables, denoting the deviating displacements from the equilibrium position of the springs L and H here, i.e. u_L and u_H . The kinetic energy T consists of two terms, as the H is taken as the coordination origin,

$$T = \frac{1}{2} \left[m_L \left(\frac{du_L}{dt} \right)^2 + m_H \left(\frac{du_H}{dt} \right)^2 \right] \quad (2)$$

The potential energy V is composed of three terms [32]: the van der Waals interaction $V_L(r_L) = V_L(d_{L0} - u_L)$, the exchange interaction $V_H(r_H) = V_H(d_{H0} + u_H)$, and the Coulomb repulsion $V_C(r_C) = V_C(d_{C0} - u_L + u_H) = V_C(d_C - u_C)$. Here, $d_{C0} = d_{L0} + d_{H0}$ is the distance between the adjacent oxygen ions at equilibrium. $d_C = d_L + d_H$ denotes that distance at quasi-equilibrium. $u_C = u_L + \Delta_L - u_H + \Delta_H$ shows the change of the distance between the two oxygen ions at quasi-equilibrium. The u_L and u_H are assumed to be of the opposite sign because of the O:H and H-O dislocate in the same direction [24]. A harmonic approximation of the potentials by omitting the higher-order terms in their

Taylor's series yields,

$$\begin{aligned}
V &= V_L(r_L) + V_H(r_H) + V_C(r_C) \\
&= \sum_n \left\{ \frac{d^n V_L}{n! dr_L^n} \Big|_{d_{L0}} (-u_L)^n + \frac{d^n V_H}{n! dr_H^n} \Big|_{d_{H0}} (u_H)^n + \frac{d^n V_C}{n! dr_C^n} \Big|_{d_C} (-u_C)^n \right\} \\
&\approx [V_L(d_{L0}) + V_H(d_{H0}) + V_C(d_C)] - V'_C u_C + \frac{1}{2} [k_L u_L^2 + k_H u_H^2 + k_C u_C^2]
\end{aligned} \tag{3}$$

where $V_x(d_{x0})$, commonly denoted E_{x0} , is the potential well depths ($n = 0$ terms) of the respective bond. Noting that the Coulomb potential never has an equilibrium point where the repulsion force is 0, we can then expand this potential at quasi-equilibrium point. Therefore, the terms of $n = 1$ is the force equaling 0 for the L and H segments at equilibrium, while equaling $-V'_C$ for the C spring at quasi-equilibrium. Here, V'_C denotes the first order derivative at the quasi-equilibrium position, i.e. $(dV_C/dr_C)_{d_C}$. The coefficients of the $n = 2$ terms, or the curvatures of the respective potentials, denote the force constants, i.e., $k_x = d^2 V_x / dr_x^2 \Big|_{d_{x0}}$ for harmonic oscillators. The $n \geq 3$ terms are the high-order nonlinear contributions that are insignificant, as it will be shown.

Substituting Eqs (2) and (3) into (1) leads to the coupled Lagrangian equation,

$$\begin{cases} m_L \frac{d^2 u_L}{dt^2} + (k_L + k_C) u_L - k_C u_H + k_C (\Delta_L - \Delta_H) - V'_C - f_P = 0 \\ m_H \frac{d^2 u_H}{dt^2} + (k_H + k_C) u_H - k_C u_L - k_C (\Delta_L - \Delta_H) + V'_C + f_P = 0 \end{cases} \tag{4}$$

A Laplace transformation [32] turns out solutions to Eq (4),

$$\begin{cases} u_L = \frac{A_L}{\gamma_L} \sin \gamma_L t + \frac{B_L}{\gamma_H} \sin \gamma_H t \\ u_H = \frac{A_H}{\gamma_L} \sin \gamma_L t + \frac{B_H}{\gamma_H} \sin \gamma_H t \end{cases} \tag{5}$$

The coefficients denote the vibrational amplitudes. γ_L and γ_H are the vibration angular frequencies of the respective segment, which depend on the force constants and the reduced masses of the oscillators [32]. This set of general solutions indicates that the O:H and the H–O segments share the same form of eigen values of stretching vibration. The force constants k_x and the frequencies ω_x are correlated as follows,

$$k_{H,L} = 2\pi^2 m_{H,L} c^2 (\omega_L^2 + \omega_H^2) - k_C \pm \sqrt{\left[2\pi^2 m_{H,L} c^2 (\omega_L^2 - \omega_H^2)\right]^2 - m_{H,L} k_C^2 / m_{L,H}} \quad (6)$$

where c is the velocity of light travelling in vacuum. Omitting the Coulomb repulsion, the coupled oscillators will be degenerated into the independent H₂O:H₂O and H–O oscillators with respective vibration frequencies of $\sqrt{k_L/m_L}$ and $\sqrt{k_H/m_H}$. With the measured ω_L and ω_H , and the known k_C , one can obtain the force constants k_x , the potential well depths E_{x0} , and the cohesive energy E_x .

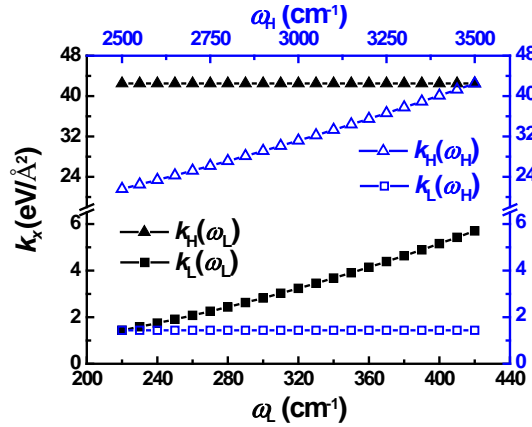


Figure 2 ω_L and ω_H dependence of the k_L and k_H with $k_C = 0.17 \text{ eV/\AA}^2$. k_L increases from 1.44 to 5.70 eV/\AA^2 while the k_H increases from 21.60 to 42.51 eV/\AA^2 as their respective frequency increases. The $k_L(\omega_H)$ and the $k_H(\omega_L)$ remains almost constant.

The force constant due to Coulomb repulsion is, $k_C = q_+ q_- / (2\pi\epsilon_r\epsilon_0 d_C^3)$ at equilibrium. Here, ϵ_r is the relative dielectric constant of ice, equaling to 3.2. $\epsilon_0 = 8.85 \times 10^{-12} \text{ F/m}$, is the vacuum dielectric

constant. The $q_e = 2e$ for the electron lone pair, and $q_c = 0.2e$ or so, is the effective charge referring to our density functional theory optimizations [32]. In this situation, the k_C equals to 0.17 eV/\AA^2 at 0 GPa. The ω_L and ω_H dependence of the k_L and the k_H , in Figure 2, shows that the k_L increases from 1.44 to 5.70 eV/\AA^2 while the k_H increases from 21.60 to 42.51 eV/\AA^2 with their respective frequency. The $k_L(\omega_H)$ and the $k_H(\omega_L)$ remains, however, almost constant. Therefore, Eq. (6) can be simplified as,

$$k_{H,L} = 4\pi^2 c^2 m_{H,L} \omega_{H,L}^2 - k_C \quad (7)$$

With the measured $\omega_L = 237.42 \text{ cm}^{-1}$ and $\omega_H = 3326.14 \text{ cm}^{-1}$ for the ice-VIII phase under the atmospheric pressure [3-6], Eq (7) derives $k_L = 1.70 \text{ eV/\AA}^2$ and $k_H = 38.22 \text{ eV/\AA}^2$. With the known $d_L = 0.1768 \text{ nm}$ and $d_H = 0.0975 \text{ nm}$ under Coulomb repulsion[24], we can obtain the free length d_{L0} is 0.1628 nm , and the d_{H0} is 0.0969 nm . Then, with the derived values of k_L and k_H , as well as the $E_{H0} = 3.97 \text{ eV}$ [32], we can determine the parameters in the van der Waals and the Morse potentials [32], as well as the force fields of the O:H–O bond at the ambient pressure,

$$\begin{cases} k_L = 72 E_{L0} / d_{L0}^2 = 1.70 \text{ eV/\AA}^2 \\ k_H = 2\alpha^2 E_{H0} = 38.22 \text{ eV/\AA}^2 \end{cases}$$

or

$$\begin{cases} E_{L0} = 1.70 \times 1.628^2 / 72 = 0.062 \text{ eV} \\ \alpha = (38.22 / 3.97 / 2)^{1/2} = 2.19 \text{ \AA}^{-1} \end{cases}$$

Using the measured [3-6, 24] Raman shifts ω_x and the interionic distances d_x [32] as input, we can readily calculate the evolution of the force constant and cohesive energy of the respective segment, from one quasi-equilibrium to another, under compression based on Eq. (6). Table 1 and Figure 3 display the results.

Results indicate that the compression shortens and stiffens the softer O:H bond, meanwhile,

lengthens and softens the H–O bond slightly through the Coulomb repulsion, which results in contraction of the O—O distance towards O:H and H–O length symmetry [3-6, 24, 33, 34]. The k_C (curvature of the Coulomb potential) in Figure 3(a), keeps almost constant under compression because of the low compressibility of O—O distance. The k_L increases more rapidly than k_H reduces because of the coupling of the compression, the repulsion, and the potential disparity of the two segments.

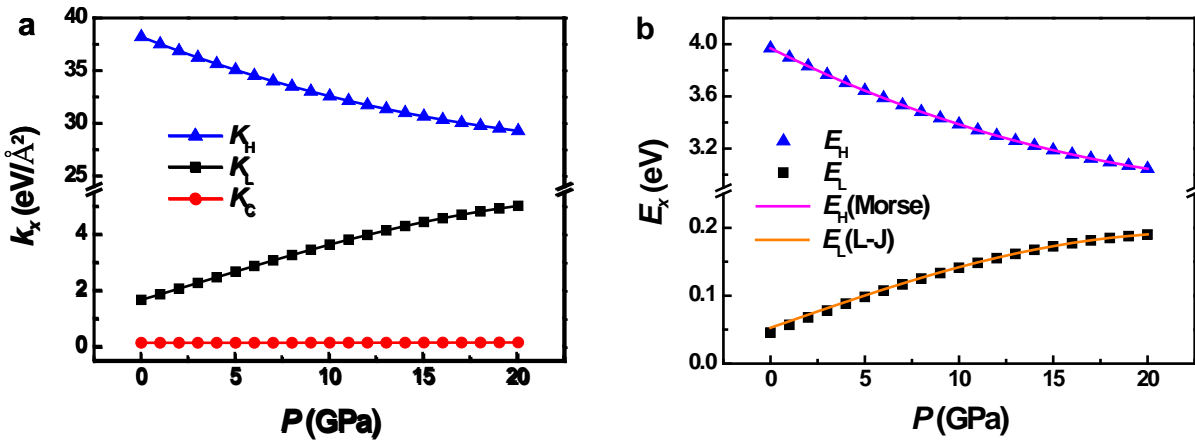


Figure 3 Pressure dependence of (a) the force constant $k_x(P)$ and (b) the cohesive energy $E_x(P)$ of the respective segment of the hydrogen bond. Solid lines in (b) results from the potential functions, which matching well the scattered data of the harmonic approximation.

As the d_L shortens by 4.3% from 0.1768 to 0.1692 nm and the d_H lengthens by 2.8% from 0.0975 to 0.1003 nm with pressure increasing from from 0 to 20 GPa [24]. Figure 3(b) indicates that the increase of pressure from 0 to 20 GPa stiffens the O:H bond from 0.046eV to 0.190 eV while soften the H–O bond from 3.97 eV to 3.04 eV. When the pressure goes up to 60 GPa, the O:H bond almost equals to the elongated H–O bond in length of about 0.110 nm, forming a symmetric O:H–O bond [3-6, 24]. At 60 GPa, the $k_L = 10.03 \text{ eV}/\text{\AA}^2$ and $k_H = 11.16 \text{ eV}/\text{\AA}^2$, the E_L recovers slightly, see Table 1. Results indicate that the nature of the interaction within the segment remains though the length and force constant approaches to equality, which means that the sp^3 -hybridized oxygen could hardly be de-hybridized by compression.

Table 1 Pressure dependence of the O:H–O segmental cohesive energy (E_x), force constant (k_x), and the stepped deviation (Δ_x) from the equilibrium position. Subscript x denotes L and H. The measured $d_x(P)$ and $\omega_x(P)$ [3-6, 24, 32] are used as input in calculations.

P (GPa)	E_L (eV)	E_H (eV)	k_L (eV/Å ²)	k_H (eV/Å ²)	Δ_L (10 ⁻² nm)	Δ_H (10 ⁻⁴ nm)
0	0.046	3.97	1.70	38.22	1.41	6.25
5	0.098	3.64	2.70	35.09	0.78	6.03
10	0.141	3.39	3.66	32.60	0.51	5.70
15	0.173	3.19	4.47	30.69	0.36	5.26
20	0.190	3.04	5.04	29.32	0.27	4.72
30	0.247	2.63	7.21	25.31	0.14	3.85
40	0.250	2.13	8.61	20.49	0.08	3.16
50	0.216	1.65	9.54	15.85	0.05	2.71
60	0.160	1.16	10.03	11.16	0.04	3.35

Figure 4 shows the E_x - d_x asymmetric relaxation dynamics of the O:H–O bond in compressed ice. The oxygen ion (solid spheres in the bottom of Figure 4) in the O:H bond moves towards while the other in the H–O bond away from the H origin. The intrinsic equilibrium position of the oxygen in H–O almost superposes on its quasi-equilibrium position, with the distance of only 6.25×10^{-4} nm. However, for O:H, the distance is 1.41×10^{-2} nm, evidencing a very soft vdW bond. The cohesive energies of both segments relax along the contours as a resultant of the Coulomb repulsion and the compression.

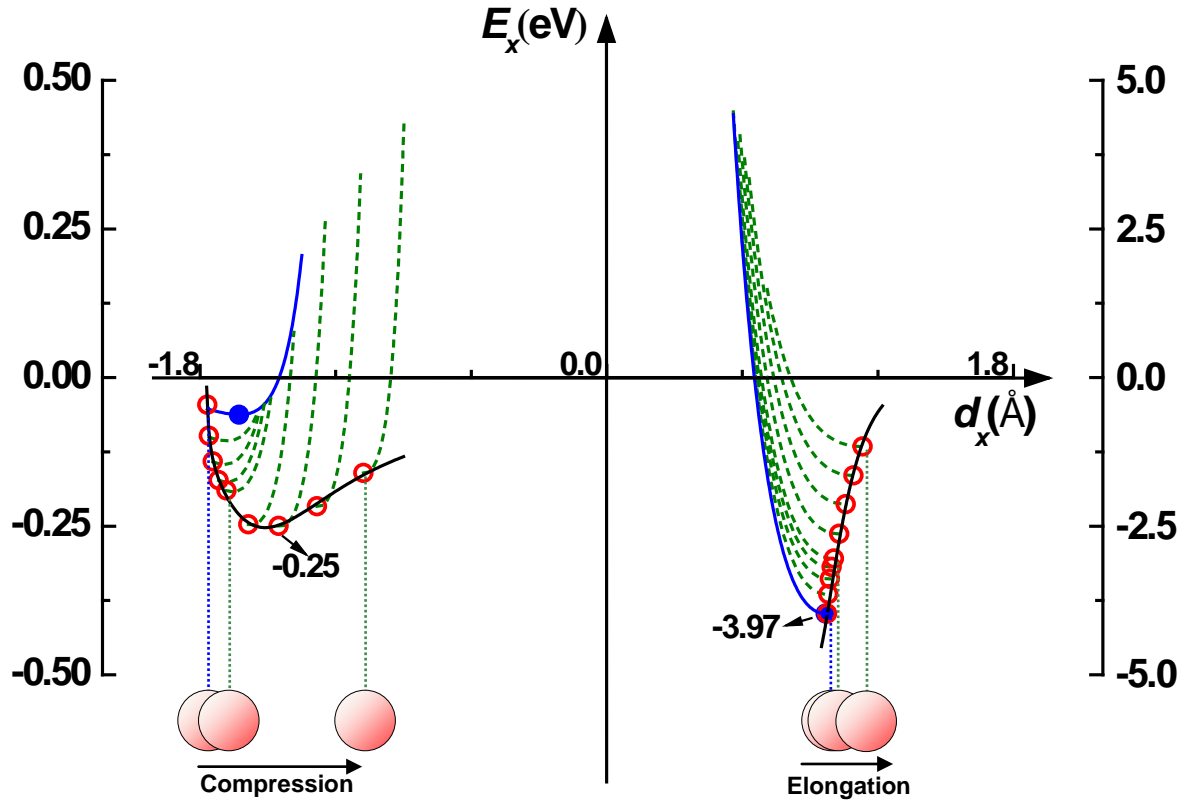


Figure 4 E_x-d_x relaxation dynamics of the O:H-O bond of compressed ice (from left to right, $P = 0, 5, 10, 15, 20, 30, 40, 50, 60$ GPa). Small solid circles in blue represent the intrinsic equilibrium coordinates (length and energy) of the oxygen without the Coulomb repulsion, and small open circles denote the quasi-equilibrium coordinates caused by both the Coulomb repulsion and the pressure. The leftmost solid (0 GPa) and the broken curves show the potentials at quasi-equilibrium while the thick solid lines are the contours of the E_x-d_x that approach the respective vdW and the Morse potential at equilibrium. Note scale difference between the two segments.

In summary, with the aid of Lagrangian-Laplace mechanics, we have been able to formulate, correlate, clarify, and quantify the short-range interactions in the flexible, polarizable hydrogen bond of compressed ice. This approach has enabled us to determine the cohesive energy, force constant, potential field of each segment and their pressure dependence based on the measurements.

Financial support from National Natural Science Foundation (No. 11172254) of China is acknowledged.

- [1] C. Medcraft, D. McNaughton, C. D. Thompson, D. R. T. Appadoo, S. Bauerecker, and E. G. Robertson, *PCCP* **15**, 3630 (2013).
- [2] V. Petkov, Y. Ren, and M. Suchomel, *J Phys: Condens Matter* **24**, 155102 (2012).
- [3] P. Pruzan, J. C. Chervin, E. Wolanin, B. Canny, M. Gauthier, and M. Hanfland, *Raman Spectrosc.* **34**, 591 (2003).
- [4] M. Song, H. Yamawaki, H. Fujihisa, M. Sakashita, and K. Aoki, *Physical Review B: Condensed Matter* **60**, 12644 (1999).
- [5] Y. Yoshimura, S. T. Stewart, M. Somayazulu, H. Mao, and R. J. Hemley, *Journal of Chemical Physics* **124**, 024502 (2006).
- [6] Y. Yoshimura, S. T. Stewart, M. Somayazulu, H. K. Mao, and R. J. Hemley, *J. Phys. Chem. B* **115**, 3756 (2011).
- [7] M. K. Tsai, J. L. Kuo, and J. M. Lu, *PCCP* **14**, 13402 (2012).
- [8] L. Pauling, *J. Am. Chem. Soc.* **57**, 2680 (1935).
- [9] G. P. Johari, and O. Andersson, *Thermochim. Acta* **461**, 14 (2007).
- [10] M. F. Kropman, H. K. Nienhuys, S. Woutersen, and H. J. Bakker, *J. Phys. Chem. A* **105**, 4622 (2001).
- [11] S. Yermenko, M. S. Pshenichnikov, and D. A. Wiersma, *Chem. Phys. Lett.* **369**, 107 (2003).
- [12] J. Alejandre, G. A. Chapela, H. Saint-Martin, and N. Mendoza, *Phys. Chem. Chem. Phys.* (2011).
- [13] C. Knight, and S. J. Singer, *J. Chem. Phys.* **129**, 164513 (2008).
- [14] R. Kumar, J. R. Schmidt, and J. L. Skinner, *J. Chem. Phys.* **126**, 204107 (2007).
- [15] C. Vega, and J. L. F. Abascal, *Phys. Chem. Chem. Phys.* **13**, 19663 (2011).
- [16] C. Wang, B. Zhou, Y. Tu, M. Duan, P. Xiu, J. Li, and H. Fang, *Sci Rep* **2**, 358 (2012).
- [17] W. G. Hant, and C. T. Zhang, *J. Phys.: Condens. Matter* **3**, 27 (1991).
- [18] T. Urbic, and K. A. Dill, *J. Chem. Phys.* **132**, 224507 (2010).
- [19] M. W. Mahoney, and W. L. Jorgensen, *J. Chem. Phys.* **112**, 8910 (2000).
- [20] P. Mark, and L. Nilsson, *J. Phys. Chem. A* **105**, 9954 (2001).
- [21] M. Agarwal, M. P. Alam, and C. Chakravarty, *J. Phys. Chem. B* **115**, 6935 (2011).
- [22] M. W. Mahoney, and W. L. Jorgensen, *J. Chem. Phys.* **115**, 10758 (2001).
- [23] D. J. Price, and C. L. Brooks, *J. Chem. Phys.* **121**, 10096 (2004).
- [24] C. Q. Sun, X. Zhang, and W. T. Zheng, *Chem Sci* **3**, 1455 (2012).
- [25] L. N. Hand, and J. D. Finch, *Analytical Mechanics* (Cambridge University Press, 2008).
- [26] H. Goldstein, *Classical Mechanics* (Addison-Wesley, 2001).
- [27] D. H. Menzel, *Fundamental formulas of physics* (Courier Dover, 1960).
- [28] C. Q. Sun, X. Zhang, X. J. Fu, W. T. Zheng, J.-L. Kuo, Y. C. Zhou, Z. X. Shen, and J. Zhou, arXiv:1210.1634.
- [29] X. Z. Li, B. Walker, and A. Michaelides, *PNAS* **108**, 6369 (2011).
- [30] R. F. McGuire, F. A. Momany, and H. A. Scheraga, *J. Phys. Chem.* **76**, 375 (1972).
- [31] N. Kumagai, K. Kawamura, and T. Yokokawa, *Mol. Simulat.* **12**, 177 (1994).
- [32] (Supplementary Information).
- [33] M. Benoit, D. Marx, and M. Parrinello, *Nature* **392**, 258 (1998).
- [34] P. Loubeyre, R. LeToullec, E. Wolanin, M. Hanfland, and D. Husermann, *Nature* **397**, 503 (1999).

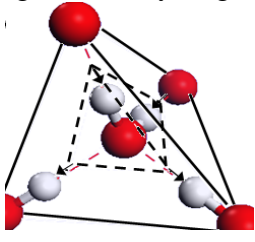
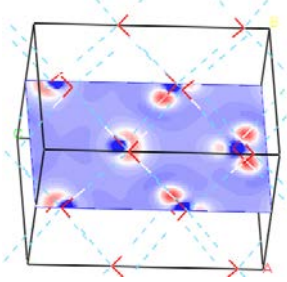
Supplementary Information

Missing short-range interactions in the hydrogen bond of compressed ice

Yongli Huang, Xi Zhang, Zengsheng Ma, Guanghui Zhou, Yichun Zhou and CQ Sun

E-mail: Ecqsun@ntu.edu.sg

1. Nomenclature

<p>(1) Segmented Hydrogen bond</p> 	<p>An expansion of Pauling's Ice Rule results the O:H–O bond that is composed of the intermolecular O:H van der Waals bond and the intramolecular H–O polar-covalent bond, rather than either of them alone [1]. This allows the inclusion of the ultra-short-range interactions discussed here.</p>
<p>(2) Electron pair repulsion</p> 	<p>DFT derived charge distribution in the cross-section of a unit cell of the ice-VIII phase [2]. Red colour represents for electron pairs and the blue for O²⁻ cores. The electron pairs are strongly and eccentrically localized.</p>

2. Potentials for the H-bond ultra-short-range interactions

The short-range interactions include the van der Waals force limited to the O:H bond [3], the exchange interaction in the H–O polar-covalent bond [4], and the Coulomb repulsion between the lone and shared electron pairs attached to the oxygen ions.

$$\left\{ \begin{array}{l} V_L(r_L) = V_{L0} \left[\left(\frac{d_{L0}}{r_L} \right)^{12} - 2 \left(\frac{d_{L0}}{r_L} \right)^6 \right] \quad (\text{Lennard - Jones potential}) \\ V_H(r_H) = V_{H0} \left[e^{-2\alpha(r_H - d_{H0})} - 2e^{-\alpha(r_H - d_{H0})} \right] \quad (\text{Morse potential}) \\ V_C(r_C) = \frac{q_+ q_-}{4\pi\epsilon_r \epsilon_0 r_C} \quad (\text{Coulomb potential}) \end{array} \right.$$

(S1)

where V_{L0} and V_{H0} , commonly denoted E_{L0} and E_{H0} , are the potential well depths of the van der Waals bond and the covalent bond, respectively. r_x and d_{x0} ($x = L, H,$ and C) denote the interionic distances (corresponding the length of the springs) at arbitrary

position and at equilibrium, respectively. α is a parameter controlling the width of the potential well. ϵ_r is the relative dielectric constant of ice, equaling to 3.2. $\epsilon_0 = 8.85 \times 10^{-12}$ F/m, is the vacuum dielectric constant. q_i and q_j denote the charges on respective oxygen ion in two segmented bonds.

With the known Coulomb potential and the measured length-stiffness relaxation parameters [2], the L-J and Morse potentials may be mathematized. Table S1 lists the expressions of the zeroth- to third-derivative of the Taylor series for L-J and Morse potentials. Table S2 gives the corresponding values (energies) of the zeroth- to third-order items evolving with the pressure. It confirms that the harmonic approximation is suitable because the 3rd item is much smaller than the 2nd item.

Table S1 The zeroth- to third-derivative of the L-J and Morse potentials

Derivative	L-J potential	Morse potential
$V_{x0}(E_{x0})$	E_{L0}	E_{H0}
V_x'	0	0
$V_x''(k_x)$	$72E_{L0}/d_{L0}^2$	$2\alpha^2 E_{H0}$
V_x'''	$-1512E_{L0}/d_{L0}^3$	$-6\alpha^3 E_{H0}$

Table S2 The values for the first four items of the Taylor series of the L-J and the Morse potentials

P (GPa)	Calculated energy (eV)							
	L-J potential				Morse potential			
	0th	1st	2nd ($\times 10^{-3}$)	3rd ($\times 10^{-3}$)	0th	1st	2nd ($\times 10^{-3}$)	3rd ($\times 10^{-3}$)
0	0.0625	0	16.8102	10.1750	3.9700	0	0.7465	0.0102
5	0.1063		8.2883	2.7002	3.6447		0.6387	0.0085
10	0.1458		4.7185	0.9904	3.3859		0.5300	0.0066
15	0.1755		2.9185	0.4391	3.1875		0.4247	0.0049
20	0.1919		1.9033	0.2212	3.0450		0.3271	0.0034
30	0.2477		0.6599	0.0397	2.6290		0.1880	0.0016
40	0.2498		0.2432	0.0089	2.1285		0.1022	0.0007
50	0.2165		0.0967	0.0024	1.6465		0.0581	0.0003
60	0.1605		0.0697	0.0017	1.1595		0.0626	0.0005

3. Lagrangian-Laplace solution

With the Lagrangian approximation, the vibration equations for O:H–O hydrogen bond can be deduced as shown in Eq.(4) in the main text.

Letting $(k_L + k_C)/m_L = a$, $(k_H + k_C)/m_H = b$, $k_C/m_L = c$, $k_C/m_H = d$,

$[k_C(\Delta_H - \Delta_L) + V'_C + f_P]/m_L = e$, $[k_C(\Delta_H - \Delta_L) + V'_C + f_P]/m_H = f$, this equation becomes,

$$\begin{cases} \frac{d^2 u_L}{dt^2} + au_L - cu_H - e = 0 \\ \frac{d^2 u_H}{dt^2} + bu_H - du_L + f = 0 \end{cases} \quad (\text{S2})$$

Assuming that the initial displacements $u_L(0)=u_H(0)=0$, and the initial velocities $du_L/dt|_{t=0} = v_{L0}$, $du_H/dt|_{t=0} = v_{H0}$. Eq. (S2) can be reorganized based on Laplace transformation,

$$\begin{cases} (s^2 + a)U_L - cU_H = v_{L0} + e/s \\ -dU_L + (s^2 + b)U_H = v_{H0} - f/s \end{cases} \quad (\text{S3})$$

where U_L and U_H are the Laplacians of the u_L and u_H , respectively, with

$$U_L = U_L(s) = \int_0^\infty u_L(t)e^{-st} dt, \quad U_H = U_H(s) = \int_0^\infty u_H(t)e^{-st} dt$$

where, s is a complex variable. Introducing $\gamma_L = \sqrt{(a+b)/2 - \lambda}$ and $\gamma_H = \sqrt{(a+b)/2 + \lambda}$, where $\lambda = \sqrt{(a-b)^2 + 4cd}/2$, we obtain the solutions to Eq. (S3),

$$\begin{cases} U_L = A_L \frac{1}{s^2 + \gamma_L^2} + B_L \frac{1}{s^2 + \gamma_H^2} \\ U_H = A_H \frac{1}{s^2 + \gamma_L^2} + B_H \frac{1}{s^2 + \gamma_H^2} \end{cases} \quad (\text{S4})$$

where

$$A_L = \frac{cv_{H0} + bv_{L0} - v_{L0}\gamma_L^2}{\gamma_H^2 - \gamma_L^2}; \quad B_L = -\frac{cv_{H0} + bv_{L0} - v_{L0}\gamma_H^2}{\gamma_H^2 - \gamma_L^2};$$

$$A_H = \frac{av_{H0} + dv_{L0} - v_{H0}\gamma_L^2}{\gamma_H^2 - \gamma_L^2}; \quad B_H = -\frac{av_{H0} + dv_{L0} - v_{H0}\gamma_H^2}{\gamma_H^2 - \gamma_L^2}.$$

These parameters denote the vibrational amplitudes.

An inverse Laplace transformation of Eq. (S4) results in Eq. (5) in the main manuscript, and the correlation between the frequency and force constants:

$$\begin{cases} \omega_{H,L} = \frac{1}{2\pi c} \left\{ \frac{1}{2m_H m_L} \left[m_H k_L + m_L k_H + (m_L + m_H)k_C \pm \sqrt{[m_L k_H - m_H k_L + (m_L - m_H)k_C]^2 + 4m_L m_H k_C^2} \right] \right\}^{1/2} \\ k_{H,L} = 2\pi^2 m_{H,L} c^2 (\omega_L^2 + \omega_H^2) - k_C \pm \sqrt{[2\pi^2 m_{H,L} c^2 (\omega_L^2 - \omega_H^2)]^2 - m_{H,L} k_C^2 / m_{L,H}} \end{cases}$$

and,

$$\begin{cases} \omega_{H,L} = \frac{1}{2\pi c} \sqrt{\frac{k_{H,L} + k_C}{m_{H,L}}} \\ k_{H,L} = 4\pi^2 c^2 m_{H,L} \omega_{H,L}^2 - k_C \end{cases}$$

by delaminating $\omega_H(k_L)$ and $\omega_L(k_H)$ that make no contribution to the cross terms.

4. DFT derived charge sharing in the H–O covalent bond of sized clusters

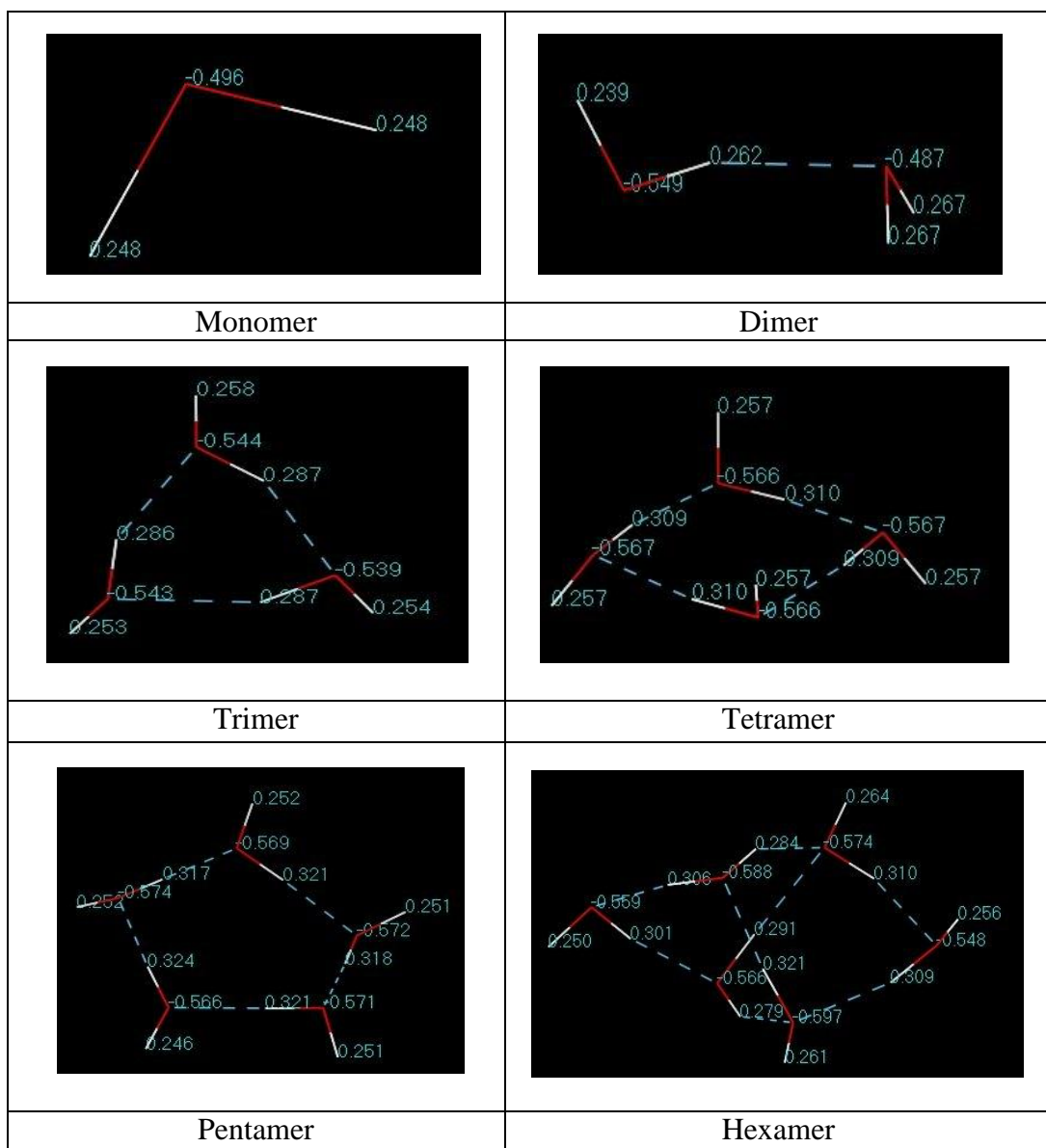


Fig. S1 DFT derived $(\text{H}_2\text{O})_N$ ($N=1-6$) charge distribution showing the charge taking by the oxygen ion in the covalent bond increases with the cluster size.

5. O:H and H-O length relaxation and the V - P curve of ice under compression [2].

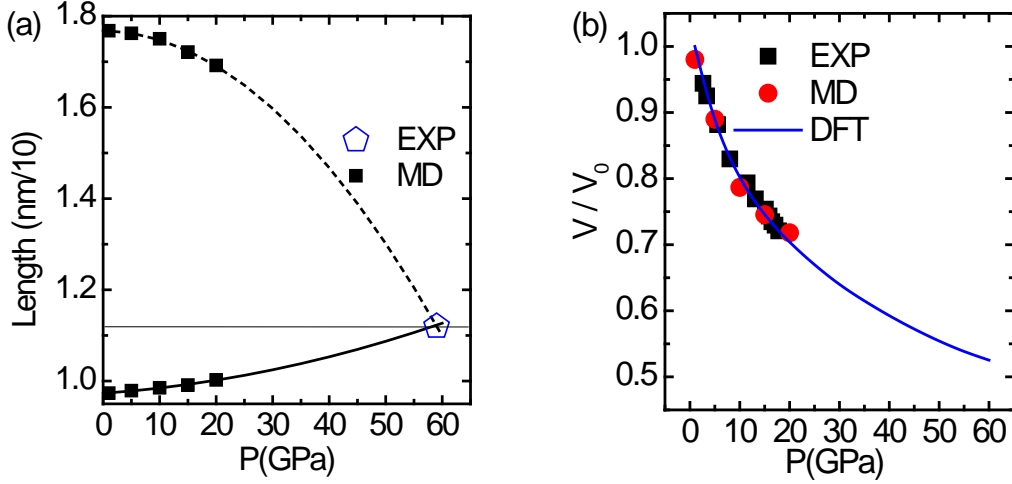


Fig.S2 (a) MD-derived O:H and H-O asymmetric relaxation dynamics and the proton centralization occurring under 58.6 GPa compression at a O---O distance of 0.221 nm agrees with measurements under 59 GPa at 0.220 nm [12, 13], which decomposes the (b) MD and DFT reproduced [14] V - P curve measurements of ice. The curves are formulated by [2]:

$$\begin{pmatrix} d_H / 0.9754 \\ d_L / 1.7683 \\ V / 1.0600 \end{pmatrix} = \begin{pmatrix} 1 & 9.510 & 2.893 \\ 1 & -3.477 & -10.280 \\ 1 & -238.0 & 47.0 \end{pmatrix} \begin{pmatrix} P^0 \\ 10^{-4} P^1 \\ 10^{-5} P^2 \end{pmatrix}$$

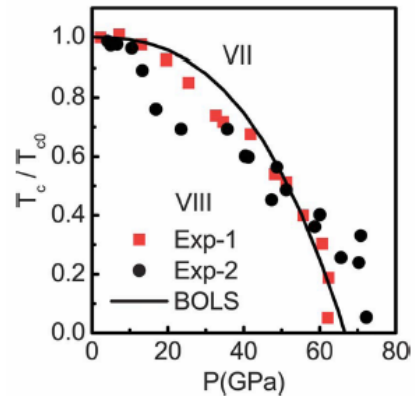
6. H-O covalent bond energy[2]

From the P -dependent critical temperature T_C for the ice VII-VIII phase transition[2], we can obtain the H-O bond energy. The relative shift in $\Delta T_C(P) = T_C(P_0) - T_C(P)$, H-O bond length (d_H) and energy (E_H) are correlated as follows[2]:

$$\frac{\Delta T_C(P)}{T_C(P_0)} = \frac{\Delta E_x(P)}{E_{x0}} = \frac{-\int_{V_0}^V p dv}{E_{H0}} = \frac{-s_0 \int_{P_0}^P p \frac{dl}{dp} dp}{E_{H0}}$$

where l can take either form of the l_L or l_H expressed in Fig. S2 caption.

As $P > P_0$, only the segment $dl_H/dp > 0$ satisfies the measured T_C - P relation that shows the pressure-depressed T_C . Assuming $s_0 = \pi \times (0.053 \text{ nm})^2$ (the cross-section area of the H-O bond), we obtained $E_{H0} = 3.97 \text{ eV}$ from fitting to the measured pressure-dependent T_C for VII-VIII phase transition[2].



7. Pressure-induced Raman shifts [15]

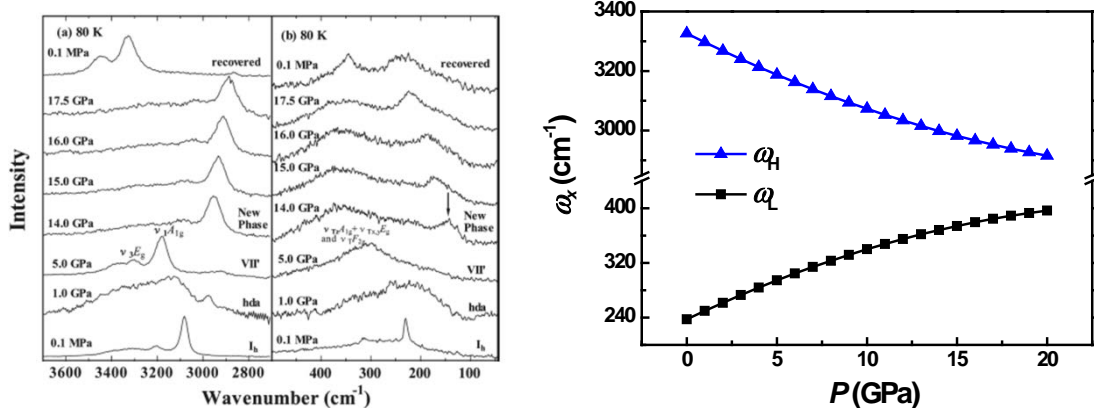


Fig S3 Raman spectra of ice-VIII measured at 80 K as a function of pressure [15], which is formulated as follow,

$$\begin{pmatrix} \omega_H / 3326.140 \\ \omega_L / 237.422 \end{pmatrix} = \begin{pmatrix} 1 & -0.905 & 1.438 \\ 1 & 5.288 & -9.672 \end{pmatrix} \begin{pmatrix} P^0 \\ 10^{-2} P^1 \\ 10^{-4} P^2 \end{pmatrix}$$

8. Pressure-dependent force constants and cohesive energies

The Lagrangian-Laplace derived force constants and cohesive energies can be formulated as:

$$\begin{pmatrix} k_H / 38.223 \\ k_L / 1.697 \end{pmatrix} = \begin{pmatrix} 1 & -1.784 & 3.113 \\ 1 & 13.045 & -15.258 \end{pmatrix} \begin{pmatrix} P^0 \\ 10^{-2} P^1 \\ 10^{-4} P^2 \end{pmatrix}$$

$$\begin{pmatrix} E_H / 3.970 \\ E_L / 0.046 \end{pmatrix} = \begin{pmatrix} 1 & -1.784 & 3.124 \\ 1 & 25.789 & -49.206 \end{pmatrix} \begin{pmatrix} P^0 \\ 10^{-2} P^1 \\ 10^{-4} P^2 \end{pmatrix}$$

- [1] L. Pauling, J. Am. Chem. Soc. **57**, 2680 (1935).
- [2] C. Q. Sun, X. Zhang, and W. T. Zheng, Chem Sci **3**, 1455 (2012).
- [3] R. F. McGuire, F. A. Momany, and H. A. Scheraga, J. Phys. Chem. **76**, 375 (1972).
- [4] N. Kumagai, K. Kawamura, and T. Yokokawa, Mol. Simulat. **12**, 177 (1994).
- [5] P. Pruzan *et al.*, Raman Spectrosc. **34**, 591 (2003).
- [6] M. Song *et al.*, Physical Review B: Condensed Matter **60**, 12644 (1999).
- [7] Y. Yoshimura *et al.*, Journal of Chemical Physics **124**, 024502 (2006).
- [8] M. A. Omar, *Elementary Solid State Physics: Principles and Applications* (Addison-Wesley, New York, 1993).
- [9] F. A. Lindemann, Z. Phys **11**, 609 (1910).
- [10] M. Zhao *et al.*, Phys Rev B **75**, 085427 (2007).
- [11] C. Q. Sun, Prog. Mater. Sci. **48**, 521 (2003).
- [12] M. Benoit, D. Marx, and M. Parrinello, Nature **392**, 258 (1998).
- [13] A. F. Goncharov *et al.*, Phys. Rev. Lett. **83**, 1998 (1999).
- [14] Y. Yoshimura *et al.*, J. Chem. Phys. **124**, 024502 (2006).

[15] Y. Yoshimura *et al.*, J. Phys. Chem. B **115**, 3756 (2011).